

Paper:

Experimental Evaluation of Highly Accurate 3D Measurement Using Stereo Camera and Line Laser

Shunya Nonaka*, Sarthak Pathak**, and Kazunori Umeda**

*Precision Engineering Course, Graduate School of Science and Engineering, Chuo University
1-13-27 Kasuga, Bunkyo-ku, Tokyo 112-8551, Japan
E-mail: nonaka@sensor.mech.chuo-u.ac.jp

**Department of Precision Mechanics, Faculty of Science and Engineering, Chuo University
1-13-27 Kasuga, Bunkyo-ku, Tokyo 112-8551, Japan
E-mail: {umeda, pathak}@mech.chuo-u.ac.jp

[Received March 13, 2023; accepted July 27, 2023]

This paper proposes a method to improve the accuracy of 3D measurement of a stereo camera by marking a measured object using a line laser. Stereo cameras are commonly used for 3D measurement, but the accuracy of 3D measurement is affected by the amount of texture. Therefore, a new measurement system combining a stereo camera and a line laser is developed. The accuracy of 3D measurement with a stereo camera is improved by using a line laser to mark arbitrary points on the measured object and measuring the marked points, regardless of the amount of texture on the measured object. Because the laser is only used to mark points on the measurement target, calibration is not required with the stereo camera. Experimental evaluation showed that our proposed method can obtain millimeters.

Keywords: 3D measurement, stereo camera, marking

1. Introduction

In recent years, 3D measurement techniques based on image processing have been utilized in various fields, such as medicine, automobiles, and architecture, and have been the subject of several studies [1–5]. These studies often used stereo cameras [6–10].

Stereo cameras use passive stereo methods for 3D measurements. Although many studies have been conducted using the passive stereo method, finding accurate corresponding points on a stereo image is difficult, and the measurement accuracy is affected by the amount of texture.

There are also active stereo methods in which one stereo camera is replaced with a light-projection device. The most representative method is the light-section (slit light projection) method [11–13]. One of the challenges of this classical method, the light-section method, is that the fixed positioning of the camera and laser can lead to blind spots. Another challenge is that the relative positions and orientations of the camera and laser must be cal-

ibrated, which is not trivial. Other methods are classified according to the type of projected light, such as spotlight projection and pattern light projection methods [14, 15]. These methods can solve the aforementioned problem of low accuracy in determining the corresponding points in stereo methods using projected light patterns. Several studies have been conducted on 3D measurements using active stereo methods. Sato et al. constructed an inspection system for automobile parts using a monocular camera and a line laser [16]. Zhao et al. proposed a method that used structured optical stripes as optical projection devices [17]. Although these are simple processes and provide mostly accurate object shape measurements, the camera and light projector must be configured precisely, and the extrinsic parameters must be calculated to obtain the overall shapes. Another issue is that the fixed positional relationship between the camera and light projector tends to create blind spots.

By contrast, Yoshimura et al. proposed a method to improve the accuracy of a stereo camera by applying handwritten markings to arbitrary welding points, even when the texture of the object being measured is small [18]. Using this method, a small stereo camera was used to acquire the 3D shapes of the marking points, and the welding points were inspected. However, their method has some problems, such as the difficulty of marking depending on the shape and size of the measured object, and the time and effort required for marking. Some studies have constructed high-precision measurement systems by combining stereo cameras and time-of-flight (TOF) range image sensors [19]. However, it was difficult to measure small objects with high accuracy in this study.

We proposed a method for obtaining 3D information with high accuracy using the principle of triangulation by marking arbitrary points on an object to be measured using a line laser and capturing images of the marked points using a stereo camera. In the method, the stereo camera needs to be fixed, but the laser can move freely; therefore, the problem of blind angles is lesser than that in the classical light section method.

The environment in which the method was applied was assumed to be indoors with controlled illumination, and



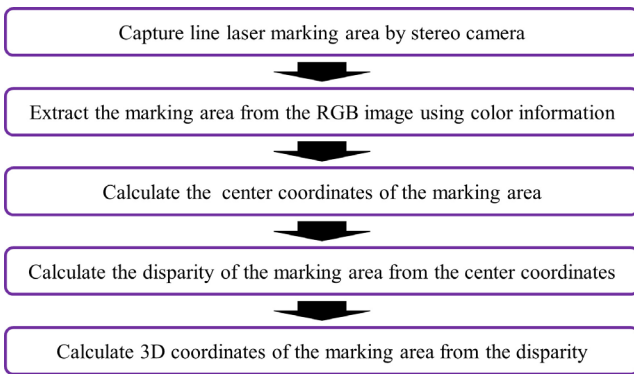


Fig. 1. Flowchart of proposed method.

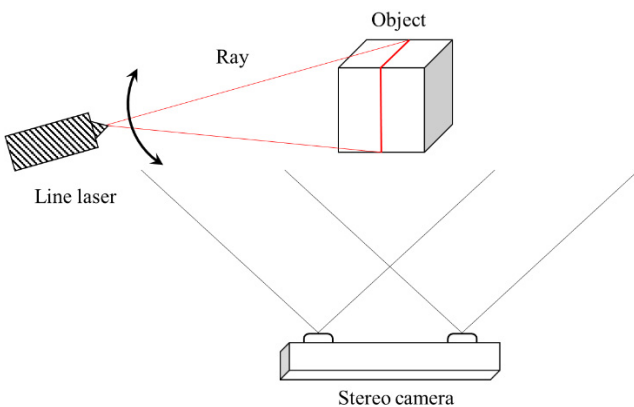


Fig. 2. System concept of proposed method.

the target objects were relatively small. The objects used in the experiments were approximately 50–200 mm in diameter. This study is attempted to inspect manufactured parts and products in a factory.

2. Proposed Method

2.1. Outline of Proposed Method

A flowchart of the proposed method is presented in Fig. 1 and a conceptual diagram of the proposed system is illustrated in Fig. 2.

First, a stereo camera was used to capture images of the measured object irradiated by a line laser at an arbitrary point. The stereo camera was fixed, and the line laser could be moved manually to the desired measurement location. Using a threshold value, the system then extracts the marking points from the color images captured by the left and right stereo cameras. The threshold value for extraction was set according to the ratio of the red, green, and blue (RGB) values of the markings in the color image. The extracted marking area has a width of several tens of pixels, and it is necessary to calculate the center coordinates on the horizontal axis of the extracted marking image to accurately calculate the 3D coordinates. In this case, the center coordinates are calculated by extracting the marked area in grayscale and using its pixel

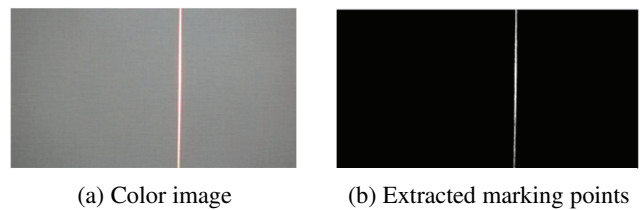


Fig. 3. Extraction of marking points.

values as weights. Subsequently, the disparity was calculated from the calculated center coordinates of the left and right images, and the 3D information of the marking area was obtained based on the principle of triangulation. The above process can be performed each time the line laser is moved to obtain the 3D information of an arbitrary area.

The essential advantage of the proposed method is that the camera and laser do not need to be calibrated. This is because the lasers are used for marking the stereo camera images, and there is no need to consider the positional relationship between the camera and laser. This means that calibration is not required, and the measurement system is hassle-free.

2.2. Detection of Marking Area

The marked area was extracted from the color image captured by the stereo camera by setting a threshold value using the RGB values or their proportions. The color of the laser was red, and the threshold was set according to the object to be measured. In the following experiments, points with $R = 255$ in the color image were extracted and measured as laser-marked points. Fig. 3 shows an image of the actual marking point extraction using a line laser.

2.3. 3D Information of Marking Area

Marking is applied with a line laser to an arbitrary point on the object to be measured. The marking area is extracted in grayscale using the threshold set in Section 2.2, and the center coordinates on the horizontal axis of the extracted marking image are calculated using the pixel values as weights for all rows. Eq. (1) was used to calculate the center coordinates x_g :

$$x_g = \frac{w_1x_1 + w_2x_2 + \dots + w_nx_n}{w_1 + w_2 + \dots + w_n} \dots \dots \dots (1)$$

where w_n is the pixel value of the grayscale image of the marking point and x_n is the x -coordinate value of the marking point.

The disparity was obtained from the calculated center coordinates of the marking area in the left and right images, and 3D information was acquired based on the principle of triangulation. Fig. 4 illustrates an example of obtaining the disparity from the left and right images. At this time, because stereo rectification is performed with the left and right cameras, the disparity is obtained between the same row coordinates in the left and right images.

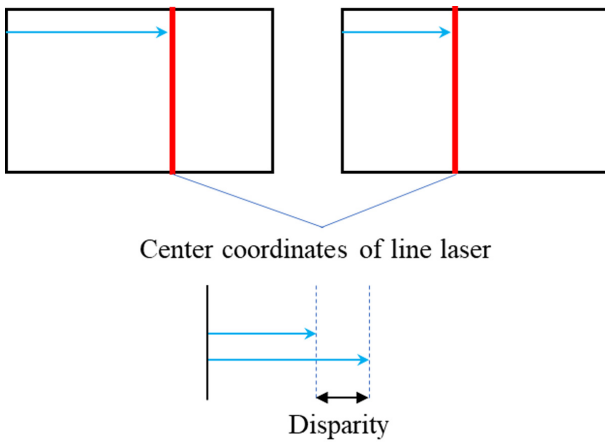


Fig. 4. Obtaining disparity.

Table 1. ZED2 distance resolution.

Measured distance [mm]	Distance resolution [mm]
300	0.711
400	1.26
500	1.97

The conversion equation from the disparity obtained in this way to three-dimensional coordinates is shown in Eqs. (2)–(4).

$$X = \frac{bx_{gn}}{S(x_{gn} - x_{gn}')} \dots \dots \dots (2)$$

$$Y = \frac{bx_{gn}'}{S(x_{gn} - x_{gn}')} \dots \dots \dots (3)$$

$$Z = \frac{bf}{S(x_{gn} - x_{gn}')} \dots \dots \dots (4)$$

where x_{gn} is the center coordinate of the laser in Line n of the left image coordinate system, x_{gn}' is the center coordinate of the laser in Line n of the right image coordinate system, f is focal length of the camera, b is the distance between the cameras, and S is the pixel size of the image pick-up device. The 3D coordinates (X, Y, Z) of the laser were based on the coordinate system of the left camera. Regarding the libraries used, stereo rectification was performed using the ZED SDK supplied with the stereo camera, while parallax calculation and transformation of the 3D coordinates were performed using OpenCV 3.14.

2.4. Target Values of Proposed Method

The numerical target in the proposed method is to maintain both the mean error and standard deviation below the sub-pixel level. The distance resolution of ZED2 is listed in Table 1 for measuring distances of 300, 400, and 500 mm, and the numerical target is to maintain the error mean and standard deviation near the values in Table 1 at each measuring distance.

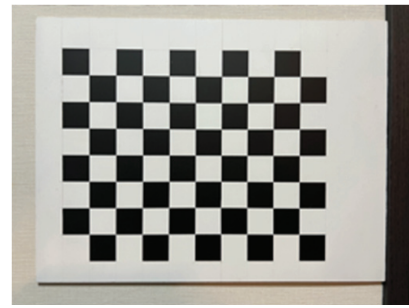


Fig. 5. Checkerboard.

3. Experiment for Accuracy Evaluation

An experiment was conducted to evaluate the accuracy of the proposed method for planar surfaces. A checkerboard was used as the plane surface, and the intersection points of the checkerboard patterns were detected to obtain a plane equation-by-plane fitting. The planes obtained by intersection detection and plane fitting were used as reference values because they provided higher accuracy than the proposed method. The accuracy of the proposed method was evaluated by calculating the error between the plane equation and the 3D information obtained by the proposed method.

3.1. Experimental Condition

As shown in Fig. 5, a checkerboard was used, with each square measuring 30 × 30 mm and ten horizontal × eight vertical squares. For plane estimation, the 3D information of the intersection points of the checkerboard was obtained using the curve-fitting toolbox in MATLAB to obtain the least-squares plane. The equation for the plane is obtained as follows:

$$ax + by + cz + d = 0. \dots \dots \dots (5)$$

The stereo camera was used as the Stereo Labs ZED2. The baseline length was 120 mm. This camera can acquire distance images via passive stereo vision using the principle of triangulation to acquire distance information only at that point by extracting laser beams from the images captured by the left and right cameras. A red-marking-line laser from an STS ML-7010 marking laser was used. The specifications of the stereo cameras and line lasers are listed in Table 2. When measuring using the proposed method, the laser is manually scanned to measure the plane, and the obtained 3D point cloud of the plane is displayed using a point cloud library [20]. In this method, the scanning interval and time were arbitrary, ensuring that the laser was visible in the camera images. However, in this experiment, the laser was scanned as perpendicular to the object as possible to facilitate the acquisition of the 3D point cloud of the target object easier to understand. In addition, shape measurement of the entire plane was performed by capturing one picture per laser position. Experiments were conducted at measurement distances of 300, 400, and 500 mm. The error was

Table 2. Experimental equipment specification.

Used equipment	Name	Specification
Stereo camera	ZED2	Image resolution: 2208 × 1242 FOV: 110° (H) × 70° (V) Baseline: 120 mm Focal length: 2.12 mm Pixel size: 2 μm
Line laser	ML-7010	Wavelength: 635 nm Class: 2 M Slit width: approximately 5 mm



(a) Corner detection (b) Plane measurement

Fig. 6. Experimental conditions.

calculated based on the distance between each point and plane.

Figure 6 shows the experimental conditions.

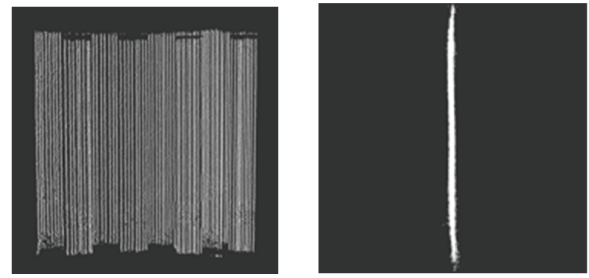
3.2. Experimental Result

The results of the proposed method are shown in **Figs. 7–9**, and **Table 3** summarizes the calculation results. The values in **Table 3** represent the errors in pixel disparity.

3.3. Discussion

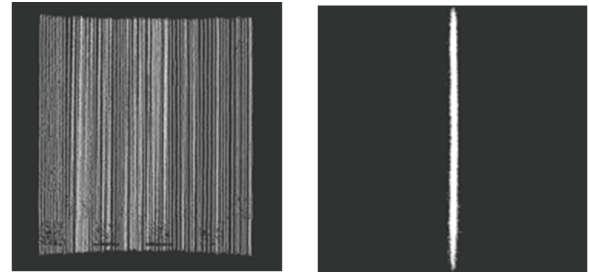
For the ZED2 stereo camera used in this experiment, the error of one pixel of disparity corresponds to 0.71 mm when the measuring distance is 300 mm, 1.26 mm when the measuring distance is 400 mm, and 1.98 mm when the measuring distance is 500 mm. The mean error and standard deviation increased as the measurement distance increased. However, the mean error was within 1 pixel and the standard deviation was within 2 pixels at all measurement distances, indicating that the proposed method provides accurate 3D measurements. The 3D point clouds obtained using the proposed method, as shown in **Figs. 7–9**, have an error of approximately 1 mm. This is thought to be because the line laser used did not have uniform brightness, which prevented proper extraction of marked points on the measured planes.

In addition, in **Figs. 7(a)** and **9(a)**, missing areas can be observed in the point clouds near the top and bottom. This was attributed to the arbitrary movement of the line laser and the performance of the line laser itself. These



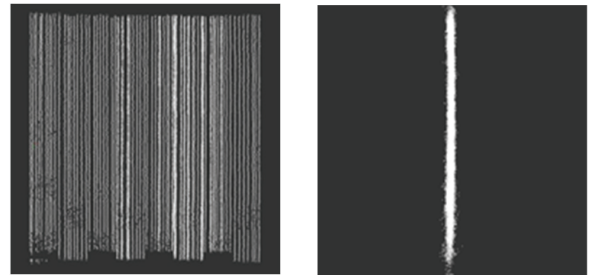
(a) Front (b) Side

Fig. 7. 3D point cloud (300 mm).



(a) Front (b) Side

Fig. 8. 3D point cloud (400 mm).



(a) Front (b) Side

Fig. 9. 3D point cloud (500 mm).

Table 3. Calculation results.

Measured distance [mm]	Mean error		Standard deviation	
	[mm]	[px]	[mm]	[px]
300	0.32	0.45	1.24	1.75
400	0.56	0.44	1.77	1.40
500	1.00	0.51	1.97	0.99

missing areas were generated in the point cloud of the measured plane owing to the vertical misalignment that occurred when moving the line laser arbitrarily and repeating the shooting multiple times. In addition, the performance of the laser was low, and the brightness was not uniform. In particular, the luminance is low at the laser edge, and light is sometimes absorbed in the black areas of the plane, making extraction difficult.

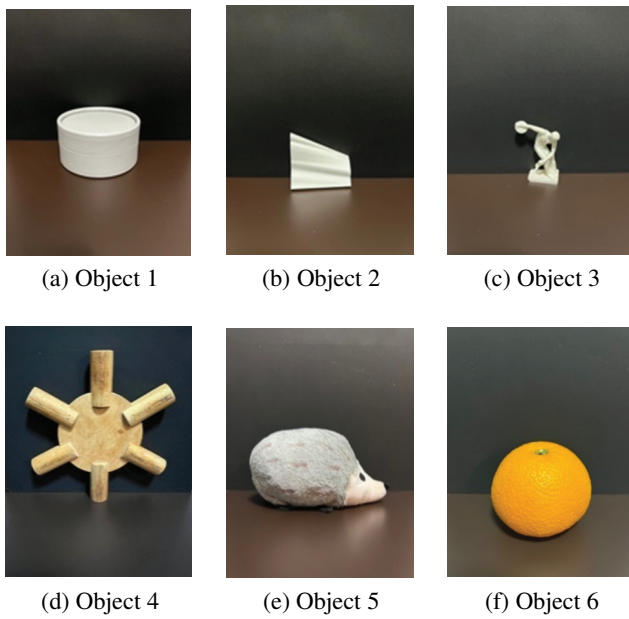


Fig. 10. Measured objects.

4. Experiment of Measuring Object Shape

Although the accuracy was evaluated using planar measurements in Section 3, it is necessary to understand the strengths and weaknesses of the proposed method by performing various shape measurements, as the actual application of this research assumes the inspection of parts and their external appearance. Therefore, 3D measurements of objects of various shapes were carried out using the proposed method and compared with the results of 3D measurements using the disparity functions of the stereo camera itself. Although no numerical comparisons have been made, shape measurements of various objects were carried out to determine whether they could be carried out successfully. This study also attempted to demonstrate the usefulness of measurements on objects with little texture.

4.1. Experimental Condition

The measurements were performed on the six types of objects shown in Fig. 10. Objects were selected because the experiment attempted to measure various shapes, and we wanted to prepare objects with simple to complex shapes and colors. The equipment and measurement methods used were the same as those described in Section 3. However, the shooting interval for obtaining the 3D point cloud of the object using the proposed method was adjusted according to the object’s size and was performed arbitrarily until the point cloud of the entire object was obtained. The three objects shown in Figs. 10(a)–(c) are a cylinder approximately 85 mm in diameter and 45-mm high, an eraser with an uneven shape approximately 50-mm high and 60 mm across, and a figure with a complex shape approximately 50-mm high and 30 mm across, all plain objects with few features. The three objects shown in Figs. 10(d)–(f) are wooden measuring ob-



Fig. 11. 3D measurement by stereo camera (Object 1).



Fig. 12. 3D measurement by stereo camera (Object 2).

jects with a height and width of approximately 180 mm, a stuffed toy with a height and width of approximately 70 and 120 mm, and a Mandarin orange with a height and width of approximately 70 and 70 mm, respectively, all of which are objects with colors and features.

When measuring with the proposed method, the illumination was dimmed to eliminate the effects of ambient light. The laser was manually scanned in the direction transverse to the object, and the entire object surface shape was acquired and displayed on the PCL by repeating the process; the results of 3D measurements made with the functions of ZED2 itself were similarly displayed on the PCL and compared in appearance, as it was difficult to compare them numerically. The measurement distance was arbitrarily set according to the size and shape of the object. The illuminance value for the measurement with the proposed method was approximately 0 lx, whereas the illuminance value for the measurement with the stereo disparity functions of ZED2 itself was approximately 100 lx. Experiments were conducted at measurement distances of approximately 300 mm for Object 1, 150 mm for Objects 2 and 3, and 400 mm for Objects 4–6.

4.2. Experimental Result

Figures 11–16 illustrate the results of the 3D measurements of each object performed by the stereo camera, and Figs. 17–22 illustrate the results of the 3D measurements of each object obtained by the proposed method.



Fig. 13. 3D measurement by stereo camera (Object 3).

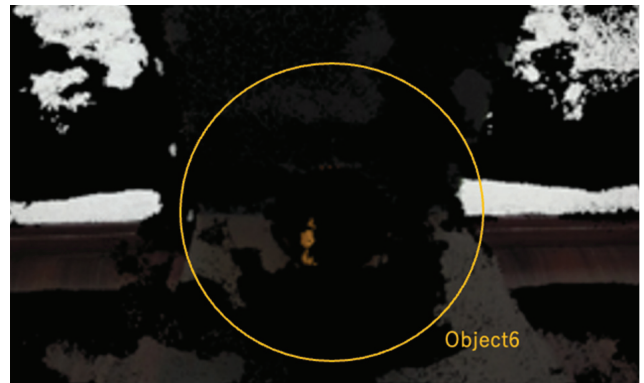


Fig. 16. 3D measurement by stereo camera (Object 6).

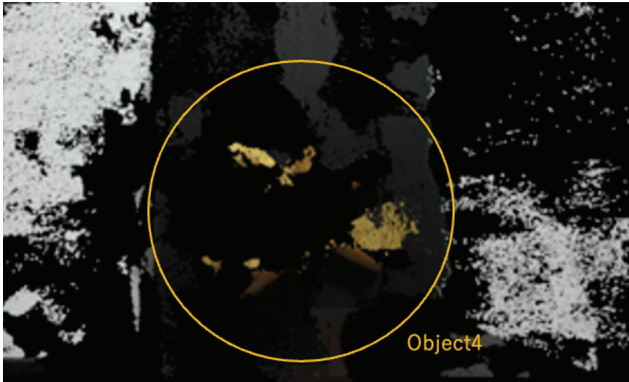


Fig. 14. 3D measurement by stereo camera (Object 4).

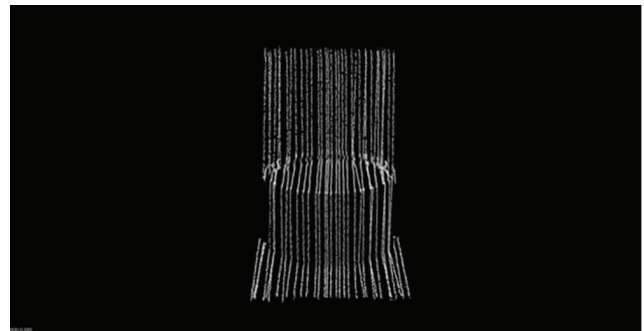


Fig. 17. 3D measurement by proposed method (Object 1).

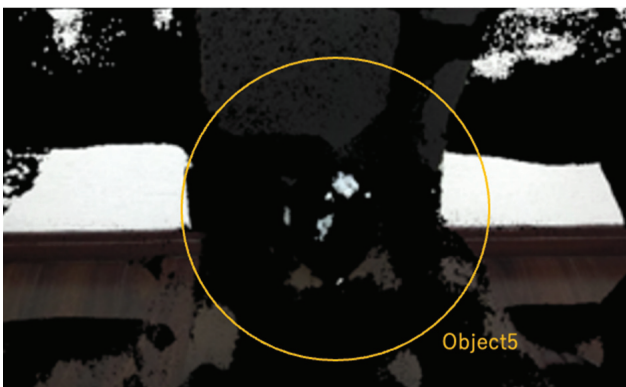


Fig. 15. 3D measurement by stereo camera (Object 5).

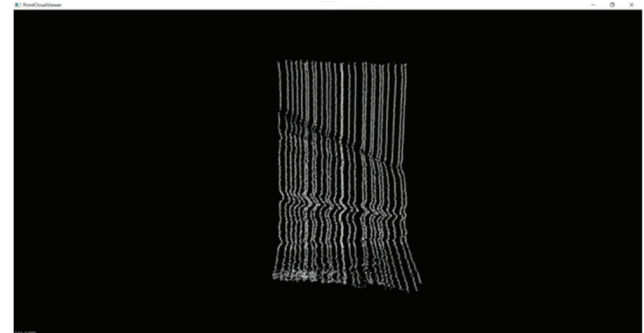


Fig. 18. 3D measurement by proposed method (Object 2).

4.3. Discussion

Figures 13–15 show that the stereo camera cannot perform 3D measurements because of the small amount of texture of the object. Figs. 14–16 illustrate that even for objects with textures, 3D measurements are difficult to achieve with a stereo camera alone.

The results of the proposed method, shown in Figs. 17–22, imply that Objects 1 and 2 could be measured in 3D shapes. However, for Object 3, it was impossible to properly measure the fine details. This is thought to be because when the line laser light hit the object, the calculation of the center coordinates did not go well because of the thick laser. 3D shape measurement was also pos-



Fig. 19. 3D measurement by proposed method (Object 3).

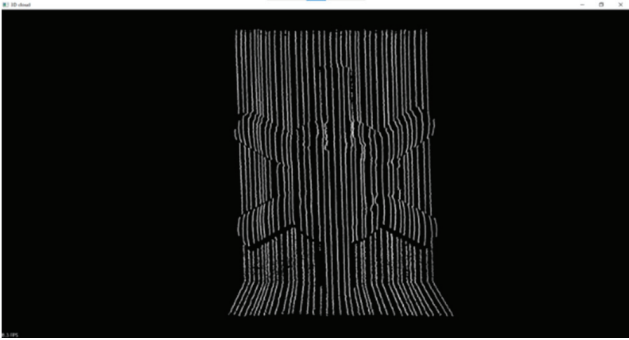


Fig. 20. 3D measurement by proposed method (Object 4).

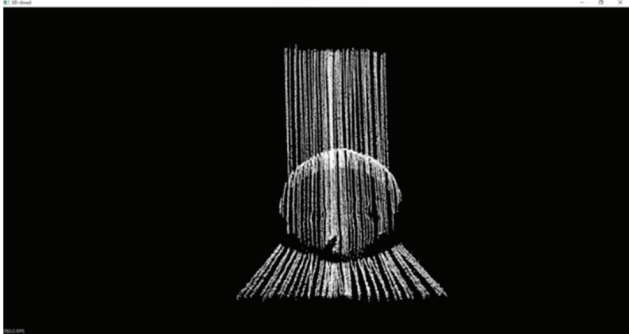


Fig. 21. 3D measurement by proposed method (Object 5).

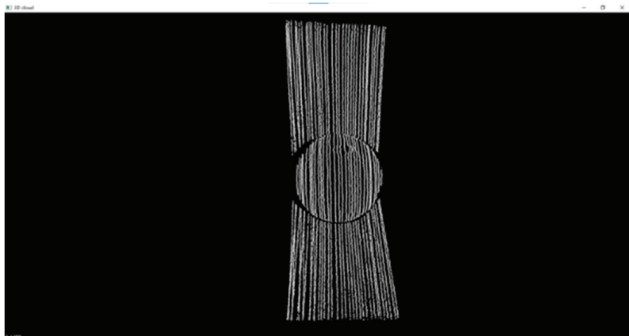
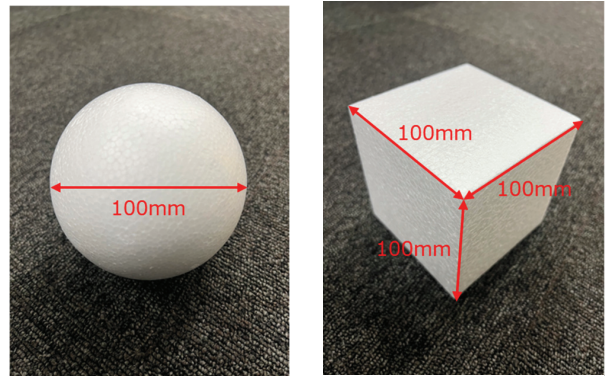


Fig. 22. 3D measurement by proposed method (Object 6).

sible for Objects 4, 5, and 6, with textures and colors. However, objects such as Object 5, which is black, absorb light when the line laser is shone on them and cannot be extracted well with the set threshold. In this case, the eyes and noses of the stuffed animals were not well extracted, indicating that they could not be measured.

Comparing the results, it can be seen that for all objects, the proposed method can acquire the shape better than the function of the stereo camera. In particular, when measuring at short distances, such as in this experiment, the function of the stereo camera cannot measure objects with features such as Objects 4, 5, and 6 because it is difficult to find the corresponding points. However, the proposed method enables 3D measurements using only set threshold values, even when the colors of the objects are different. One possible reason is that the colored objects



(a) Sphere (b) Cube

Fig. 23. Measured objects.

measured in this experiment did not contain many colors that easily absorb light, such as black and dark blue. It is also considered that even differently colored objects can be extracted because the brightness of the line laser used causes even colored objects to appear similarly.

5. Experiment of All-Round 3D Measurement

Using the proposed method, all-round 3D measurements were performed on two types of objects—a sphere and a cube—using a rotating table. The accuracy of each measurement is evaluated. This experiment attempted to demonstrate the usefulness of the proposed method by quantitatively evaluating the results of the shape measurements, in contrast to the shape measurements of the objects in Section 4, which were evaluated based on their appearance. In addition, because the aim is to measure the entire surface of the object in the future, the evaluation in this experiment used 3D point clouds obtained by all-round shape measurements on a rotating table.

5.1. Experimental Condition

All-round 3D measurements were performed on the two types of objects shown in Fig. 23; each object was a Styrofoam sphere with a diameter of 100 mm and a Styrofoam cube with one side of 100 mm.

The measurements were performed in an aluminum frame, as shown in Fig. 24, in an environment where the influence of ambient light was eliminated by applying a dark curtain. The illuminance of the experimental environment was approximately 5 lx. The turntable in Fig. 25 was placed before the stereo camera. The object was rotated every 90°, the laser was scanned laterally to the object, and the process was repeated to obtain a 3D point cloud of the object’s surface at each angle. The point cloud is then integrated with each object to obtain a point cloud for the entire circumference. The shooting distance is approximately 350 mm.

The obtained point clouds of all-round shapes were subjected to shape detection using the free 3D point-cloud processing software CloudCompare [a] and were

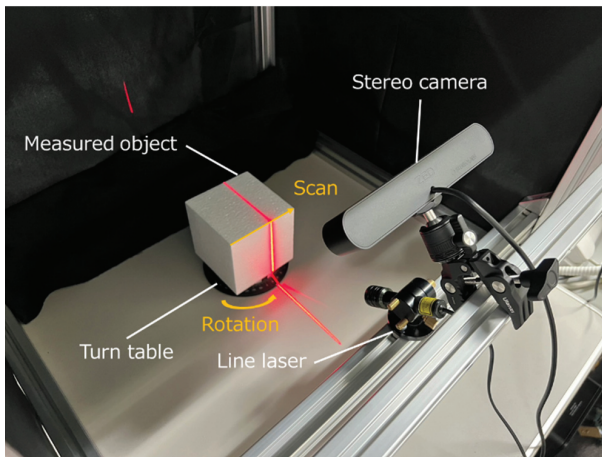


Fig. 24. Experiment conditions.



Fig. 25. Turntable.

evaluated for accuracy. RANSAC Shape Detection [21] within CloudCompare was used for the shape detection. It uses the automatic shape-detection algorithm proposed by Ruwen et al., which can estimate models from data containing outliers by eliminating their effects. It estimates six planes for spheres and cubes and evaluates their accuracy. To evaluate the accuracy, the sphere was averaged by calculating the difference between the estimated sphere radius R and the distance d from the center of the sphere, which was estimated using the point cloud obtained by the proposed method as the error, as shown in Fig. 26. For the cubes, the distance between each estimated plane and the point cloud of each plane using the proposed method was calculated as the error and averaged.

5.2. Experimental Result

The results of applying RANSAC Shape Detection to the point cloud results measured by the proposed method with rotations of 0° , 90° , 180° , and 270° , the all-surrounding shape point cloud obtained by integrating them and the integrated all-surrounding shape point cloud are shown in Figs. 27 and 28 for the sphere and cube, respectively. The results of the error calculations are listed in Table 4, the diameter dimensional error of the sphere in Table 5, the dimension error of each plane of the cube

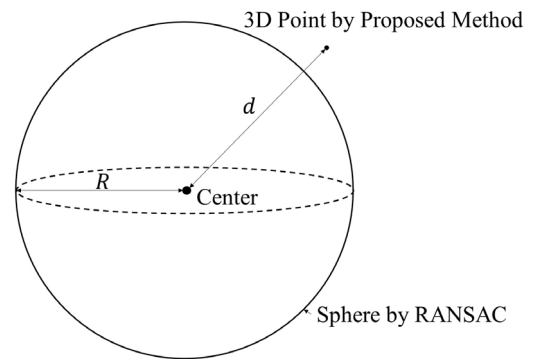
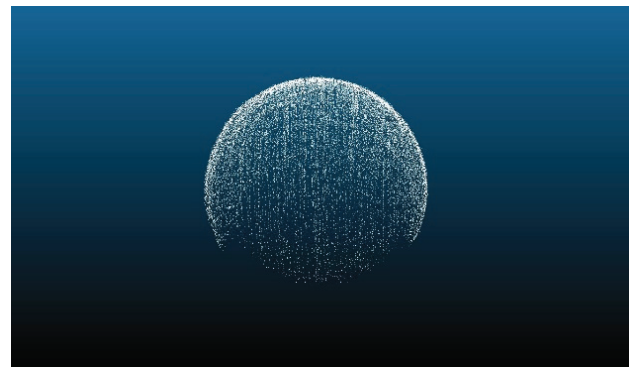
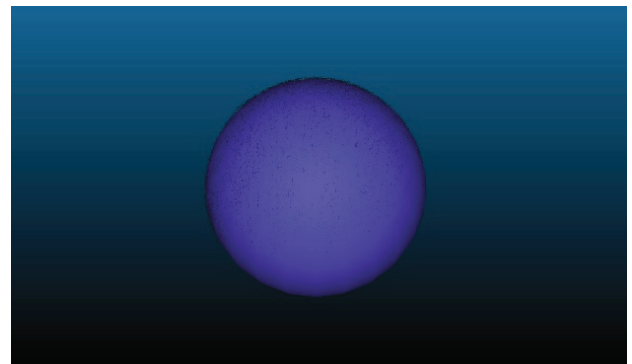


Fig. 26. Error of sphere.



(a) Sphere (integration)



(b) Sphere (RANSAC Shape Detection)

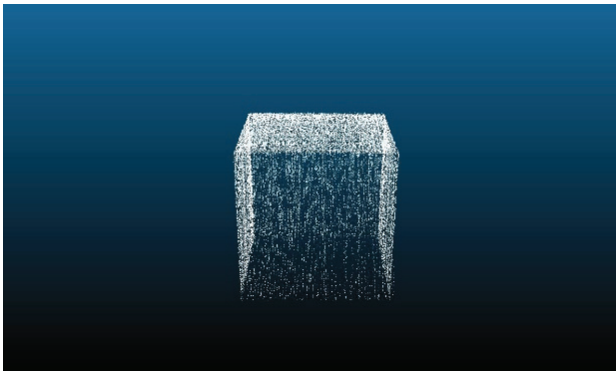
Fig. 27. 3D measurement by proposed method (sphere).

in Table 6, the parallelism of the opposing planes of the cube in Table 7, and the angles of the adjacent faces of the cube in Table 8.

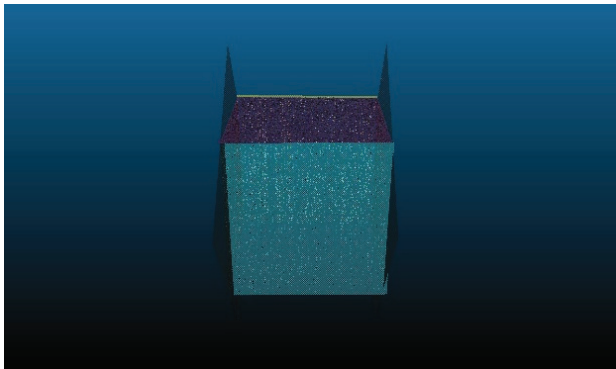
5.3. Discussion

Figures 27(a) and (b) illustrate that RANSAC Shape Detection can be successfully applied to the point cloud of the integrated all-surrounding shape in a sphere to estimate the shape. Similarly, Figs. 28(a) and (b) illustrate that the five measured planes can be successfully estimated in the cube.

This is because the 3D measurement was performed properly at all angles, and it can be said that the mea-



(a) Cube (integration)



(b) Cube (RANSAC Shape Detection)

Fig. 28. 3D measurement by proposed method (cube).

Table 4. Calculation results.

	Mean error [mm]	Standard deviation [mm]
Sphere	-0.001	0.074
Cube (front)	0.024	0.103
Cube (top)	0.031	0.051
Cube (back)	0.022	0.153
Cube (left)	0.024	0.020
Cube (right)	0.023	0.066

surement was successful.

However, for the cube, as shown in **Fig. 28(a)**, some gaps could be observed at the corners, and the entire circumference shape could not be obtained. This is thought to be because the laser width of the line laser used in this experiment was approximately 5 mm; therefore, even if the line laser was applied to the corner part, it deviated from the corner when the center coordinates were calculated. This is thought to be improved by changing the line laser to one with a smaller laser width or by irradiating the line laser vertically and horizontally to the object, as in this experiment.

Table 4 indicates that very accurate 3D measurements with an error average of -0.001 mm can be made on a sphere. This is thought to be because the sphere has no

Table 5. Diameter dimension error of sphere.

	Error [mm]
Sphere	-0.254

Table 6. Dimensional error of each plane of cube.

	Error of height [mm]	Error of width [mm]
Cube (front)	0.279	-0.198
Cube (top)	0.095	0.121
Cube (back)	0.209	0.065
Cube (left)	0.421	-0.097
Cube (right)	0.439	0.076

Table 7. Parallelism of opposing planes of cube.

	Parallelism [°]
Front and back	1.49
Left and right	1.29

Table 8. Calculation results.

	Angle [°]
Front and top	89.28
Front and right	89.80
Front and left	89.91
Right and top	89.30
Right and back	90.51
Back and top	90.60
Back and left	90.58
Left and top	90.59

corners, and even a line laser with a laser width of about 5 mm, such as that used in this experiment, can be irradiated and extracted uniformly. In the case of the cube, the error average was about 0.025 mm in any plane, and high-precision 3D measurement was achieved. The standard deviation is also less than 0.2 mm for both spheres and cubes.

Table 5 indicates that the diameter error of the sphere is -0.254 mm, and **Table 6** stipulates that the dimensional error of each cube plane is within ±0.5 mm in any plane, each error within 1%, indicating that highly accurate measurement was achieved.

Table 7 indicates that the parallelism of the opposing planes is about 1.5° each. The slight inclination is thought to be because the measurement accuracy is degraded because the measurement distance varies slightly from plane to plane during rotation.

Table 8 stipulates that the angles of the adjacent planes

of the cube are within $90^\circ \pm 1^\circ$ in all adjacent planes, indicating that accurate measurements are being made.

6. Conclusion

This study proposed a method to improve the accuracy of 3D measurements by marking with a stereo camera and a line laser.

Experiments were conducted to assess the accuracy of the proposed method using a checkerboard plane. Hence, highly accurate 3D measurements were achieved at all measurement distances of 300 mm, 400 mm, and 500 mm. In the object shape measurement experiments, three plain objects with few features and three colored objects with features were measured using the proposed method. The effectiveness of the proposed method was confirmed by comparing the results with the results of 3D measurement using the functions of the ZED2 stereo camera itself. The results demonstrate that the proposed method provides more accurate 3D measurements for all objects than 3D measurements using stereo camera functions. In the all-surrounding shape measurement experiment, two objects—a sphere and a cube—were rotated using a turntable, and the overall shape of the object's surface was acquired using the proposed method. Accuracy evaluations were then performed using the 3D point-cloud processing software CloudCompare. It was confirmed that highly accurate measurements were achieved for both the spheres and cubes.

As a prospect, at the present stage, line laser extraction is made easier by dimming the lighting and installing a dark screen during measurement; however, we would like to make it possible to robustly extract laser marking points even in scenes affected by ambient light and other factors. To achieve this, it is necessary to devise methods for estimating appropriate thresholds. In addition, as the proposed method involves offline measurements, we would like to enable online measurements. In addition, we intend to construct an online measurement system that considers the rotation angle in all surrounding geometry measurements using a rotating table.

References:

- [1] E. Heo, M. Kwon, and B. Kim, "Large free form measurement using slit beam," 2008 Int. Conf. on Control, Automation and Systems, Seoul, South Korea, pp. 1224-1227, 2008. <https://doi.org/10.1109/ICCAS.2008.4694335>
- [2] S. Ding, X. Zhang, H. Chen, and J. Wang, "Large scale object's measurement method research based on multi-view reconstruction," 2017 2nd Int. Conf. on Image, Vision and Computing (ICIVC), Chengdu, pp. 555-558, 2017. <https://doi.org/10.1109/ICIVC.2017.7984617>
- [3] Z. Liu, J. Huang, S. Bu, J. Han, X. Tang, and X. Li, "Template Deformation-Based 3-D Reconstruction of Full Human Body Scans From Low-Cost Depth Cameras," IEEE Trans. on Cybernetics, Vol.47, No.3, pp. 695-708, 2017. <https://doi.org/10.1109/TCYB.2016.2524406>
- [4] S. Gao, C. F. Cheung, and D. Li, "Autostereoscopic Measurement System for Rapid 3D Inspection of Wire Bonding," 2021 Int. Conf. of Optical Imaging and Measurement (ICOIM), Xi'an, China, pp. 145-148, 2021. <https://doi.org/10.1109/ICOIM52180.2021.9524422>
- [5] M. Kawata, H. Higuchi, S. Pathak, A. Yamashita, and H. Asama,

"Scale Optimization of Structure from Motion for Structured Light-based All-round 3D Measurement," 2021 IEEE Int. Conf. on Systems, Man, and Cybernetics (SMC), Melbourne, Australia, pp. 442-449, 2021. <https://doi.org/10.1109/SMC52423.2021.9658793>

- [6] M. Yao and B. Xu, "A Dense Stereovision System for 3D Body Imaging," IEEE Access, Vol.7, pp. 170907-170918, 2019. <https://doi.org/10.1109/ACCESS.2019.2955915>
- [7] D. Hong, H. Lee, M. Kim, and H. Cho, "A 3D inspection system for PCB board by fusing moiré technique and stereo vision algorithm," SICE Annual Conf. 2007, Takamatsu, pp. 2473-2479, 2007. <https://doi.org/10.1109/SICE.2007.4421405>
- [8] A. Harjoko, R. M. Hujja, and L. Awaludin, "Low-cost 3D surface reconstruction using Stereo camera for small object," 2017 Int. Conf. on Signals and Systems (ICSIGSYS), Bali, Indonesia, pp. 285-289, 2017. <https://doi.org/10.1109/ICSIGSYS.2017.7967057>
- [9] H. Aoki, T. Shiga, A. Suzuki, and K. Takeuchi, "Non-contact Heart-beat Measurement by Hybrid Method of Passive Stereo and Active Stereo," 2019 IEEE 1st Global Conf. on Life Sciences and Technologies (LifeTech), Osaka, Japan, pp. 115-116, 2019. <https://doi.org/10.1109/LifeTech.2019.8883983>
- [10] A. Okubo, A. Nishikawa, and F. Miyazaki, "Selective reconstruction of a 3-D scene with an active stereo vision system," Proc. of Int. Conf. on Robotics and Automation, Albuquerque, NM, USA, Vol.1, pp. 751-758, 1997. <https://doi.org/10.1109/ROBOT.1997.620125>
- [11] Y. Shirai, "Recognition of polyhedrons with a range finder," Pattern Recognit., pp. 243-244, 1972. [https://doi.org/10.1016/0031-3203\(72\)90003-9](https://doi.org/10.1016/0031-3203(72)90003-9)
- [12] H. Sasama, "Evaluation of Slit Light System for Objects with Metallic Reflection and Application to Iron Wheels," J. Robot. Mechatron., Vol.10, No.5, pp. 455-461, 1998. <https://doi.org/10.20965/jrm.1998.p0455>
- [13] O. Ozeki, K. Kogure, H. Onouchi, H. Higuchi, and S. Yamamoto, "Visual Inspection System for Welded Beads of Automotive Panel," J. Robot. Mechatron., Vol.5, No.2, pp. 112-116, 1993. <https://doi.org/10.20965/jrm.1993.p0112>
- [14] H. Kijima and H. Oku, "Structured Light Field by Two Projectors Placed in Parallel for High-Speed and Precise 3D Feedback," J. Robot. Mechatron., Vol.34, No.5, pp. 1096-1110, 2022. <https://doi.org/10.20965/jrm.2022.p1096>
- [15] J. Chen, Q. Gu, T. Aoyama, T. Takaki, and I. Ishii, "Blink-Spot Projection Method for Fast Three-Dimensional Shape Measurement," J. Robot. Mechatron., Vol.27, No.4, pp. 430-443, 2015. <https://doi.org/10.20965/jrm.2015.p0430>
- [16] R. Sato, K. Kato, and K. Harada, "Development of the hole position inspection system of pressed car parts by using laser 3-d measurement," The 19th Korea-Japan Joint Workshop on Frontiers of Computer Vision, Incheon, South Korea, pp. 317-322, 2013. <https://doi.org/10.1109/FCV.2013.6485513>
- [17] L. Zhao, H. Xu, J. Li, and Q. Cai, "Binocular Stereo Vision Measuring System Based on Structured Light Extraction Algorithm," 2012 Int. Conf. on Industrial Control and Electronics Engineering, Xi'an, China, pp. 644-647, 2012. <https://doi.org/10.1109/ICICEE.2012.174>
- [18] M. Yoshimura, Y. Ji, and K. Umeda, "Stereo Measurement of Cross-Sectional Shape of Weld Beads by Marking," 2020 ICPE 18th Int. Conf. on Precision Engineering, D-4-5, 2020.
- [19] T. Fukuda, Y. Ji, and K. Umeda, "Accurate Range Image Generation Using Sensor Fusion of TOF and Stereo-based Measurement," Proc. 12th France-Japan and 10th Europe-Asia Congress on Mechatronics, 2018. <https://doi.org/10.1109/MECATRONICS.2018.8495739>
- [20] R. B. Rusu and S. Cousins, "3D is here: Point Cloud Library (PCL)," IEEE Int. Conf. on Robotics and Automation (ICRA), 2011. <https://doi.org/10.1109/ICRA.2011.5980567>
- [21] R. Schnabel, R. Wahl, and R. Klein, "Efficient RANSAC for Point-Cloud Shape Detection," Computer Graphics Forum, Vol.26, No.2, pp. 214-226, 2007. <https://doi.org/10.1111/j.1467-8659.2007.01016.x>

Supporting Online Materials:

- [a] CloudCompare version 2.12.4, GPL Software, 2023. <http://www.cloudcompare.org/> [Accessed December 1, 2022]



Name:
Shunya Nonaka

Affiliation:
Precision Engineering Course, Graduate School of Science and Engineering, Chuo University

Address:
1-13-27 Kasuga, Bunkyo-ku, Tokyo 112-8551, Japan

Brief Biographical History:
2022 Received B.Eng. in Precision Mechanics from Chuo University

Membership in Academic Societies:
• The Japan Society of Mechanical Engineers (JSME)



Name:
Sarthak Pathak

ORCID:
0000-0002-5271-1782

Affiliation:
Assistant Professor, Department of Precision Mechanics, Chuo University

Address:
1-13-27 Kasuga, Bunkyo-ku, Tokyo 112-8551, Japan

Brief Biographical History:
2014 Received Bachelor of Technology and Master of Technology degrees from Department of Engineering Design, Indian Institute of Technology, Madras (IITM)
2017 Received Ph.D. degree from Department of Precision Engineering, The University of Tokyo
2017- Postdoctoral Researcher, Department of Precision Engineering, The University of Tokyo
2018- JSPS Postdoctoral Research Fellow, Department of Precision Engineering, The University of Tokyo
2020- Project Assistant Professor, Department of Precision Engineering, The University of Tokyo
2021- Assistant Professor, Department of Precision Mechanics, Chuo University

Main Works:
• S. Pathak, A. Moro, H. Fujii, A. Yamashita, and H. Asama, "Spherical Video Stabilization by Estimating Rotation from Dense Optical Flow Fields," J. Robot. Mechatron., Vol.29, No.3, pp. 566-579, 2017.
• D. Kim, S. Pathak, A. Moro, A. Yamashita, and H. Asama, "Self Supervised Optical Flow Derotation Network for Rotation Estimation of a Spherical Camera," Advanced Robotics, Vol.35, Issue 2, pp. 118-128, 2021.
• S. Pathak, A. Moro, A. Yamashita, and H. Asama, "A Decoupled Virtual Camera Using Spherical Optical Flow," Proc. of the 2016 IEEE Int. Conf. on Image Processing (ICIP 2016), pp. 4488-4492, 2016.

Membership in Academic Societies:
• Institute of Electrical and Electronics Engineers (IEEE)
• The Japan Society for Precision Engineering (JSPE)
• The Robotics Society of Japan (RSJ)



Name:
Kazunori Umeda

ORCID:
0000-0002-4458-4648

Affiliation:
Professor, Department of Precision Mechanics, Chuo University

Address:
1-13-27 Kasuga, Bunkyo-ku, Tokyo 112-8551, Japan

Brief Biographical History:
1994 Received Ph.D. in Precision Machinery Engineering from The University of Tokyo
1994- Lecturer, Department of Precision Mechanics, Chuo University
2003-2004 Visiting Worker, National Research Council of Canada
2006- Professor, Department of Precision Mechanics, Chuo University

Main Works:
• M. Shinozaki, M. Kusanagi, K. Umeda, G. Godin, and M. Rioux, "Correction of color information of a 3D model using a range intensity image," Computer Vision and Image Understanding, Vol.113, No.11, pp. 1170-1179, 2009.
• T. Kuroki, K. Terabayashi, and K. Umeda, "Construction of a Compact Range Image Sensor Using Multi Slit Laser Projector and Obstacle Detection of a Humanoid with the Sensor;" 2010 IEEE/RSJ Int. Conf. on Intelligent Robots and Systems (IROS2010), pp. 5972-5977, 2010.
• S. Yan, S. Pathak, and K. Umeda, "PointpartNet: 3D point cloud registration via deep part based feature extraction," Advanced Robotics, Vol.36, Issue 15, pp. 724-734, 2022.

Membership in Academic Societies:
• The Robotics Society of Japan (RSJ)
• The Japan Society for Precision Engineering (JSPE)
• The Japan Society of Mechanical Engineers (JSME)
• The Society of Instrument and Control Engineers (SICE)
• The Institute of Electronics, Information and Communication Engineers (IEICE)
• Institute of Electrical and Electronics Engineers (IEEE)
